RSC Advances




ROYAL SOCIETY OF CHEMISTRY

www.rsc.org/advances

# Design of ultra-sensitive gold nanorods colorimetric sensor and its application based on formaldehyde reducing $Ag^+$

Jin-Mei Lin [a], Yi-Qun Huang [a, b], Zhen-bo Liu [c], Chang-Qing Lin[d], Xudong Ma[b], Jia-Ming Liu [a,*]

[a] College of Chemistry and Environmental, Minnan Normal University, Zhangzhou, 363000, P.R. China

[b] Zhangzhou Affiliated Hospital of Fujian Medical University, Zhangzhou, 363000, P.R. China

[c] The third Hospital of Xiamen, Xiamen, 361000, PR China

[d] Department of Food and Biological Engineering, Zhangzhou Institute of Technology, Zhangzhou, 363000, P.R. China

**Abstract** Formaldehyde (HCHO) could reduce $Ag^+$ to Ag on the surface of gold nanorods (AuNRs) to form Au core-Ag shell nanorods (Au@AgNRs) in AuNRs-$Ag^+$-HCHO system, which caused dielectric function to change, longitudinal plasmon absorption band (LPAB) of AuNRs to redshift ($\Delta\lambda_{LPAB}$) and the color of the solution to change obviously. Thus, a responsive, simple, sensitive and selective AuNRs colorimetric sensor for the determination of HCHO has been developed based on the linear relationship between $\Delta\lambda_{LPAB}$ and the concentration of HCHO. The limit of detection (LOD) of this sensor is $6.3\times10^{-11}$ (g $mL^{-1}$), which is much lower than that of surface-enhanced raman spectroscopy (SERS), showing its high sensitivity. What's more, the sensor has been applied to the detection of HCHO in water samples with the results agreeing well with resonance fluorescence spectrometry, showing its great practicality. Furthermore, the morphological changes of AuNRs and Au@AgNRs were characterized by transmission electron microscope (TEM) and the sensing mechanism for the detection of HCHO was also discussed.

**Keywords** Formaldehyde; Gold nanorods; colorimetric sensor; Au core-Ag shell nanorods

## 1.Introduction

The effects of HCHO on human body are well known: irritations of eye and upper respiratory tract,

* Corresponding author: Tel.:+86 596 2591352.
E-mail address: zzsyliujiaming@163.com (J. Liu).

headache, nausea, drowsiness and allergic skin reactions [1]. It is also a potential mutagen and carcinogen in laboratory animal tests for its serious toxicological properties [2]. The World Health Organization (WHO) determined that the concentration of HCHO in residential indoor areas must not exceed 82 ppb (parts per billion) [3]. Rapid methods are suitable for the analysis of large numbers of samples on-site in order to obtain accurately and timely analysis results, especially in environmental concerns [4]. Therefore, it is essential to develop rapid methods for the accurate determination of trace HCHO in environmental water samples.

Many analytical methods have been reported for the determination of HCHO in various samples, including spectrophotometry [5], fluorimetry [6], capillary chromatography [7], flow injection catalytic method [8], voltammetry [9], solid substrate-room temperature phosphorimetry (SSRTP) [10], resonance fluorescence spectrometry [11], chemiluminescence[12], gas chromatography (GC) [13], catalytic fluorescence method [14], SERS [15], HPLC [16], conductometric biosensor [17], gas sensor [18], low-temperature sensor [19] and miniature room temperature sensor [20]. However, these methods are either expensive, labor intensive or time consuming, making them unsuitable for on-site analysis.

To overcome these difficulties, colorimetric methods have been actively pursued because they can be easily read out with naked eye but any specific instrument. In the past two decades, much attention has been focused on the gold nanoparticles-based visual detection methods due to their simplicity, sensitivity as well as the potential application to on-site detection [21-23]. Gold nanorods (AuNRs) have gained increased attention in colorimetric sensor because their longitudinal LPAB band is highly sensitive to minute changes in the AuNR aspect ratio (length/width) [24-25]. Compared with spherical gold nanoparticles, AuNRs possess more fantasticality properties in optics and electrics [26]. Moreover, the synthesis method is simple and its yield can be as high as 97% [27, 28] and their color changes are more sensitive to the changing of size dimension and surrounding medium [29]. Especially, AuNRs possess two plasmon absorption bands: LPAB and transverse plasmon absorption band (TPAB). Thereinto, the location of LPAB mainly depends on the shape, surface charge and dielectric conditions of AuNRs [30].

Taking advantage of these characteristics, lots of AuNPs colorimetric sensors have been developed for the detection of ions ($Hg^{2+}$ [31], Cr (VI) [32], $NO_2^-$ [33], $S^{2-}$ [34], $Pb^{2+}$ [35], $I^-$ [36], $Cu^{2+}$ [37], $Fe^{3+}$ [38], $Co^{2+}$ [39]), biomolecules (cysteine and glutathione [40], cysteine [41], dopamine [42], vitamin C [43]) and organic molecules (endotoxin [44], cholinesterase and organophosphate pesticides [45] and glucose [46]). The mentioned above sensors can be distinguished as aggregation sensors based on

cross-linking and electrostatic absorption. However, most of these analyte-induced aggregation colorimetric sensors display drawbacks in terms of actual applicability. For exemple, the cross-linking colorimetric sensors have to synthesize the cross-linking agent possessing at least two binding sites in order to connect individual AuNPs; the aggregation colorimetric sensor needs surface modification and troublesome operation. Therefore, it is imperative to develop an easy-handled, cost-effective and environmentally-friendly colorimetric sensor for HCHO on-spot detection.

In this work, we describe a novel AuNRs colorimetric sensor developed based on the linear correlation of the $\Delta\lambda_{LPAB}$ with the concentration of HCHO and the color of the solution to obviously change. These findings have innovations in fabricating AuNRs sensor and colorimetric analysis. For example, for the detection of HCHO, SERS was proposed based on derivatization reaction tween 4-amino-5-hydrazino-3-mercapto-1,2,4-triazole and HCHO [15], while the AuNRs colorimetric sensor was designed based on the the linear correlation of the $\Delta\lambda_{LPAB}$ with the $C_{HCHO,}$ and AuNRs colorimetric sensor has the new breakthrough in methodology; the proposed sensor for the detection of HCHO which was achieved with simple visual inspection in less than 15 min, is expected to be used for on-line analysis, while SERS method is either time consuming and laborious and unsuitable for on-site analysis; the sensitivity of this sensor (LOD: $6.3\times10^{-11}$ g $mL^{-1}$) is 2.4 times higher than that of SERS method (LOD: $1.5\times10^{-10}$ g $mL^{-1}$), and to our knowledge, AuNRs colorimetric sensor for the detection of HCHO has not been reported yet.; this rapid, accurate, selective and repeatable sensor has been applied to determine trace HCHO in water samples; showing better application prospects.

## 2. Experimental

### 2.1 Instrumentation and chemicals

Absorption spectra were recorded using a UV-2550 spectrophotometer (Shimadzu, Japan). TEM was performed on a JEM-1230 electron microscope (JEOL, Ltd., Japan) at 300 kV.

Formaldehyde working solution: 0.27 mL of 37%-40% HCHO (AR, Chengdu Chemical Reagent Plant) was transferred to a 100 mL volumetric flask, diluted with water. The concentration was calibrated by iodimetry, and then diluted to 1.00 μg $mL^{-1}$ with water as stock solution,. it was gradually diluted to 10.00 and 100.00 (ng $mL^{-1}$) as HCHO working solutions before use. $HAuCl_4\cdot3H_2O$ (>99%), $AgNO_3$ (>99%), $NaBH_4$ (99%), L-ascorbic acid (>99%), salicylic acid (>99%), hexadecyl trimethyl ammonium bromide (CTAB, 99%), NaOH and glycine were from Sinopharm Chemical Reagent Co.,

Ltd (Shanghai, China). Doubly-distilled water (18.2 MΩ) was used in all experiments.

The experiment and sample analysis were conducted in cleaning room with an air-conditioner. The Heal-power multifunctional paint, which can wipe off formaldehyde by 98%, was painted on the inner-wall and on the ceiling.

2.2 Synthesis of AuNRs

AuNRs were synthesized according to an improved silver ion-assisted seed-mediated method previously reported by Ye et al. [28].

In brief, the seed solution was prepared by mixing 5.00 mL of 0.20 M CTAB and 5.00 mL of 0.020 mM $HAuCl_4$ upon stirring vigorously in a flask. Thereafter, 0.60 mL of 0.010 M $NaBH_4$ (ice-cold) was added, and the color of the solution changed from dark yellow to brownish yellow under vigorously stirring, indicating the formation of seed solution. After vigorously stirring for 2 min, the seed solution was kept in a water bath at 30 °C for at least 1 h before use.

To prepare the growth solution, 3.60 g CTAB and 0.32 g salicylic acid were dissolved with 100 mL warm water in a flask. Cooled the solution to 30 °C, 2.40 mL of 4.0 mM $AgNO_3$ solution was added and kept undisturbed at 30 °C for 15 min. Then 100 mL of 1.0 mM $HAuCl_4$ was added and vigorously stirred for 15 min, afterwards 0.50 mL of 0.10 M Vc was added and finally the growth solution was obtained.

0.32 mL seed solution was taken out and added to the growth solution with continuously stirring for 30 s. The solution was aged at 30 °C for 12 h to ensure the full growth of AuNRs. Then AuNRs solution was obtained for use.

2.3. Experimental method

1.00 mL AuNRs, 85 μL of 0.010 M $AgNO_3$ and different concentrations of HCHO were added to a 10.0-mL colorimetric tube, then pH value was adjusted to 9.58 with 0.050 M glycine-sodium hydroxide buffer solution and diluted to 10.0 mL with water. After a quick mixing, the solution was incubated at 50 °C for 15 min and then kept in ice-water bath for 5 min to stop the reaction completely. At the same time, the reagent blank experiment was also carried out. Finally, absorption spectra of the system were scanned and the redshift ($\Delta\lambda_{LPAB} = \lambda_1 - \lambda_2$). was calculated (the LPAB of test solution ($\lambda_2$) and reagent blank ($\lambda_1$) were recorded, respectively).

## 3. Results and discussion

### 3.1. Sensing strategy

In order to investigate the sensing mechanism for the detection of HCHO, the UV–vis absorption spectra of AuNRs-$Ag^+$-glycine-sodium hydroxide buffer-HCHO system was scanned (**Fig. 1**, **Table 1**).

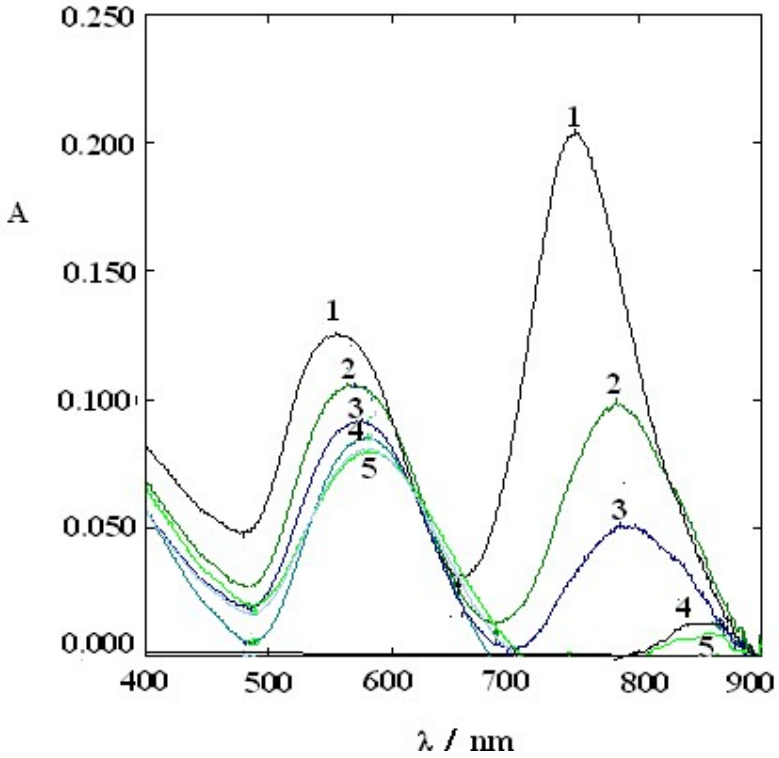


**Fig. 1.** UV-Vis absorption spectra of AuNRs-$Ag^+$-glycine-sodium hydroxide buffer-HCHO system containing 1.00 mL AuNRs, 85.0 μL of 0.010 M $AgNO_3$ and 1.00 mL glycine-sodium hydroxide buffer when concentrations of HCHO were 0, 2.00, 40.00, 80.00 and 140.00 (ng) at 50 ˚C for 15 min

**Table 1** UV-Vis characteristics of AuNRs-$Ag^+$-glycine-sodium hydroxide buffer-HCHO system

| System | $\lambda_{LPAB}$ (nm) | Amax (ΔA) | $\lambda_{TPAB}$ ( nm) | Amax (ΔA) |
|---|---|---|---|---|
| 1. 1.00 mL AuNRs + 85.0 μL $Ag^+$ + 1.00 mL glycine-sodium hydroxide buffer | 748 | 0.204 | 555 | 0.125 |
| 2. 1 + 2.00 ng HCHO | 782 (34) | 0.099 (0.105) | 564 (9) | 0.106 (0.019) |
| 3. 1 + 40.00 ng HCHO | 786 (38) | 0.052 (0.152) | 576 (21) | 0.092 (0.033) |

| | | | | |
|---|---|---|---|---|
| 4. 1 + 80.00 ng HCHO | 837 (49) | 0.016 (0.188) | 580 (25) | 0.085 (0.040) |
| 5. 1 + 140.00 ng HCHO | 853 (65) | 0.001 (0.203) | 583 (28) | 0.081 (0.044) |

As shown in **Fig. 1**, there are two major absorption bands of AuNRs located at 748 nm for LPAB and at 555 nm for transverse plasmon absorption band (TPAB) in AuNRs-$Ag^{+}$-glycine-sodium hydroxide buffe solution, respectively. HCHO added to the AuNRs-$Ag^{+}$-glycine-sodium hydroxide buffer solution system, the LPAB of AuNRs underwent a redshift, the reason contributed to that $Ag^{+}$ was reduced to $Ag^{0}$ by HCHO [47], which wrapped up on the surface of AuNRs to form Au@Ag↓NRs (**Scheme 1**).

$$HCHO + Ag^{+} \longrightarrow Ag^{0} + HCOOH \quad (1)$$

$$AuNRs + Ag^{0} \longrightarrow Au@Ag\downarrow NRs \quad (2)$$

**Scheme 1.** Forming of Au@Ag↓NRs: (1) is reacting equations between HCHO and $Ag^{+}$; (2). $Ag^{0}$ is wrapped up on the surface of AuNRs to form Au@Ag↓NRs

.

Comparison TEM images of AuNRs (**Fig. 2a**) and Au@Ag↓NRs (**Fig. 2b**), can observe the AuNRs surface with a layer of bright part, this is because the deposition of Ag on the surface of AuNRs due to the $Ag^{+}$ was reduced to $Ag^{0}$ by HCHO [48], which is deposited on the surface of AuNRs and forming a Au@Ag↓NRs (**Scheme 1**). In this sensing system, HCHO could reduce $Ag^{+}$ to Ag, which selectively deposited on the tips of AuNRs to form Au@Ag↓NRs due to the shielding effect of the surfactant CTAB on the transverse site of AuNRs. As a result, caused the aspect ratio and the morphology of AuNRs were changed. For example, the length of initial AuNRs was 20-30 nm (**Fig. 2a,** The structure of the cuboid), while length of AuNRs was 40-50 nm with the addition of HCHO (**Fig. 2b,** The structure of the dumbbell). The morphology and size changes of AuNRs effectively proved the formation of Au@Ag↓NRs in the presence of HCHO in AuNRs-$Ag^{+}$-glycine –sodium hydroxide buffer system.

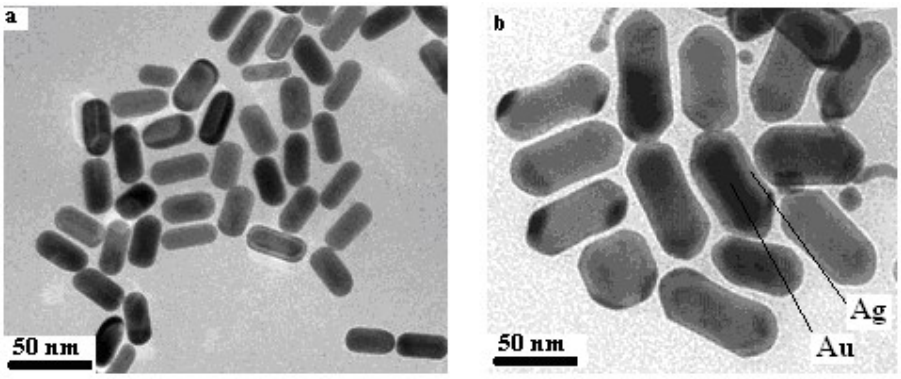


**Fig.2** TEM images of (a) AuNRs and (b) Au@Ag↓NR

As the concentration of HCHO increases, the LPAB of AuNRs gradually redshift (**Fig. 1**) and the color of the solution to change obviously (**Fig. 3**). The phenomenon could be explained as the formation of Au@Ag↓NRs due to the deposition of Ag on the surface of AuNRs. With further increasing the thickness of Ag shell, the dielectric environment around AuNRs was changed, caused overall aspect ratio (length/width) of AuNRs and $\Delta\lambda$ of LPAB to increase gradually [49]. What's more, the AuNRs-$Ag^{+}$-glycine-sodium hydroxide buffer system had rapid response to HCHO, and the linear relationship existed between $\Delta\lambda_{LPAB}$ and the concentration of HCHO with correlation coefficient (r) of 0.9948. The reason might be that at the tips of gold nanorods Au-Ag energy binding is lower that on the side, and thus when the Ag approach the gold nanorod surface, reduction at the sides is hindered and tip coating is the most favorable mechanism [50]. The effects of different depositional model on the the optical properties of gold nanorods are not the same [50]. For complete coverage type, the absorbance of LPAB decreases tempestuously, but the displacement is very small; for cutting-edge coverage type, the absorbance of LPAB decreases is not only attenuated tempestuously, accompanied by obvious redshift. Thus, HCHO could be detected using AuNRs colorimetric sensor. Sensing mechanism for HCHO detection as shown in **Scheme 2.**

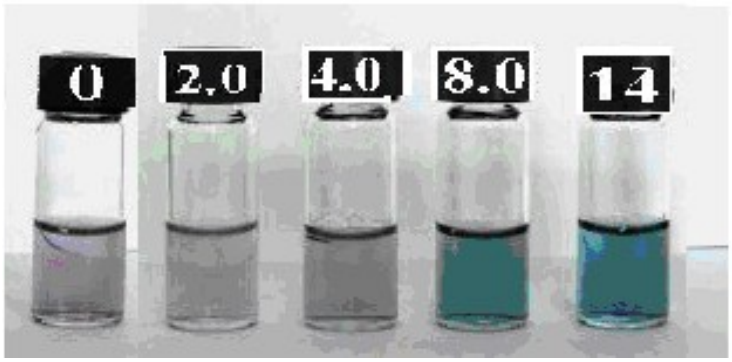


**Fig. 3.** Color responses when AuNRs react with HCHO of various concentrations (0, 20, 40, 80 and 140 (ng/10 mL)) after incubation at 50 °C for 15 min under the condition of pH = 9.58, 1.00 mL AuNRs, 85.0 μL of 0.01 M $AgNO_3$ and 1.00 mL glycine-sodium hydroxide buffe

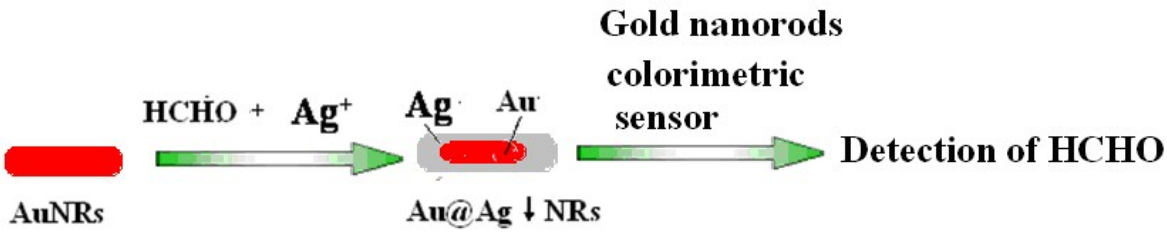


**Scheme 2.** Sensing mechanism for colorimetric determination of HCHO

3.2. Optimum measurement condition

For the system containing 8.0 ng HCHO $mL^{-1}$, a number of parameters that influence on the sensitivity, selectivity, accuracy and stability of AuNRs colorimetric sensor were investigated in a univariate approach.

3.2.1. Effect of the pH of the system

HCHO has the ability to reduce metal ions to metal nanoparticles under the alkaline condition [51]. At the same time, $Ag^+$ could react with glycine to form complex which could be to prevent the formation of AgCl and AgBr precipitates [49]. Thus, the pH of the system was adjusted by adding NaOH-glycine buffer solution. **Fig. S1** show that the $\Delta\lambda_{LPAB}$ increased with the increasing of pH, mainly because HCHO has the strong ability to reduce $Ag^+$ under the alkaline condition; the $\Delta\lambda_{LPAB}$ reached maximum when the pH of the system was 9.58, because the strongest reducibility was highest under this condition;

the $\Delta\lambda_{LPAB}$ decreased when the pH of the system exceeded 9.58, which attributed to the fact that with the increasing of pH the yield of AgOH show an increasing tendency, weakening the reaction between HCHO and $Ag^{+}$. For the reason mentioned above, glycine-sodium hydroxide buffer of pH 9.58 was chosen as the optimum reaction media.

3.2.2. Effects of the dosage of AuNRs and $AgNO_3$

The effects of the dosage of AuNRs and $AgNO_3$ on the $\Delta\lambda_{LPAB}$ of the system were examined. The concentration of AuNRs was estimated by assuming a 100% synthetic yield. As shown in **Fig. S2A**, when the dosage of AuNRs was 0.60 mL the $\Delta\lambda_{LPAB}$ of the system reached the peak value but narrow linear range, while high dosage caused too small $\Delta\lambda_{LPAB}$. According to the change of $\Delta\lambda_{LPAB}$ and linear range, 1.00 mL was chosen as the optimal dosage of AuNRs. The effect of the dosage of 0.010 M $AgNO_3$ on the $\Delta\lambda_{LPAB}$ is shown in **Fig. S2B**. The $\Delta\lambda_{LPAB}$ enhanced gradually when the dosage of $AgNO_3$ was in the range of 10-150 μL, the reason was that the rising of $AgNO_3$ dosage caused the thickness of Ag shell on the surface of AuNRs to enhance and the aspect ratio of AuNRs to increase. Because $Ag^{+}$ could react with $Br^{-}$ in CTAB to form AgBr precipitate, which caused concentration of $Ag^{+}$ in the solution to reduce quickly and ability of reduction reaction between $Ag^{+}$ and HCHO to reduce. Thus, 85.0 μL was chosen as the optimal dosage of $AgNO_3$.

3.2.3. Effects of reaction temperature and time

The effects of the temperature and time on the $\Delta\lambda_{LPAB}$ of the system were investigated according to the experimental method. Results show that the $\Delta\lambda_{LPAB}$ increased with the increasing of reaction temperature and reached the maximum at 50 °C; when the temperature exceeded 50 °C the $\Delta\lambda_{LPAB}$ decreased (**Fig. S3A**) because of the thermal reshaping of AuNRs under high temperature [52]. At the same time, the $\Delta\lambda_{LPAB}$ increased gradually with the increasing of the reaction time due to the increasing of the yield of Au@Ag NRs, and the $\Delta\lambda_{LPAB}$ reached the maximum at 15 min, indicating that the yield of Au@Ag NRs maximum (**Fig. S3B**). Taking these factors into account, 50 °C and 15 min were chosen as the optimal reaction conditions in the following studies.

3.2.4. Stability of sensor

Under the experiment conditions described above, the effects of the standing time on the $\Delta\lambda$ of system were examined in order to evaluate the stability of this sensor. When the standing time of the

system were 5, 10, 15, 20, 25 and 30 min after cooled with running water for 5 min, the Δλ of the system were 49, 49, 49, 49, 49 and 49, respectively, the corresponding RSD% were 3.0, 3.1, 3.0, 3.0, 3.1 and 3.1 (**Fig. S4**), indicating that the sensor has good stability.

Taking these factors into account, the conditions of pH = 9.58,1.00 mL AuNRs, 85.0 μL of 0.010 M $AgNO_3$ and 1.00 mL glycine-sodium hydroxide buffe reacted at 50 °C for 15 min were chosen as the optimal condition for the detection of HCHO.

3.3. Analytical parameters

As shown in **Fig. S5,** under the optimal conditions,. the linear range, the regression equation of working curve, correlation coefficient (r), RSD % (RSD is calculated from the determining results for the samples containing 0.20 and 14.00 ($\times10^{-9}$, g $mL^{-1}$) for 6 times, respectively), the LOD (calculated by 3Sb/k, there into, 3Sb/k referred to the quotient between triple of the blank reagent's standard deviation and the slope of the working curve; Sb referred to the standard deviation of 11 parallel analysis of the blank reagent) and limit of quantification (LOQ, it is calculated by 10Sb/k) of this AuNRs colorimetric sensor were compared with those in Ref. [15], and the results are listed in Table 2. As shown in **Table 2**, both the AuNRs colorimetric sensor and the SSRTP have high sensitivity, while the SSRTP has higher sensitivity than the AuNRs colorimetric sensor, but it is either time consuming and laborious as well as unsuitable for on-site analysis. The proposed sensor has higher sensitivity than the SERS method, and it is expected to be used for on-site analysis of HCHO in real samples with low content.

**Table 2** Comparison of analysis methods

| Method | Concentrations of HCHO (g $mL^{-1}$) | Regression equation (g $mL^{-1}$) | r | RSD (%) | LOD (g $mL^{-1}$) | LOQ (g $mL^{-1}$) |
|---|---|---|---|---|---|---|
| AuNRs colorimetric sensor | 0.20-14.0 ($\times10^{-9}$) | $\Delta\lambda_{LPAB} = 32.11 + 2.273 \times10^{-9}C_{HCHO}$ ($n = 6$) | 0.9942 | 4.2-3.1 | $6.3\times10^{-11}$ | $2.1\times10^{-10}$ |
| SSRTP [10] | 0.040-4.0($\times10^{-12}$) | $\Delta I_p = 1137.2 + 1.1$ | 0.9986 | 3.0-4.2 | $1.1 \times 10^{-14}$ | |

| | | | | | | |
|---|---|---|---|---|---|---|
| | | $\times 10^{-11} C_{HCHO}$ | | | | |
| Resonance fluorescence spectrometry [11] | 0.02-1.20 ($\times 10^{-6}$) | $F = 123.0 + 2.8\times 10^{-3} C_{HCHO}$ | 0.9994 | 2.6-2.2 | $6.1\times 10^{-9}$ | |
| Catalytic fluorescence method [14] | 0–0.3 ($\times 10^{-6}$) | $\Delta F = 8.46 + 2.17\times 10^{-3} C$ | 0.9991 | 2.0-2.2 | $2..0 \times 10^{-7}$ | $6.7\times 10^{-7}$ |
| SERS [15] | 1–1,000 ($\times 10^{-9}$) | $\Delta I_{SERS,\ 1s} = 79867 + 7.2\times 10^{-7}$ C | 0.9993 | | $1.5 \times 10^{-10}$ | |
| HPLC [16] | 0.046-4.6 ($\times 10^{-6}$) | $A = 7.65 + 6.9 \times 10^{-4} C$ | 0.9998 | | $1.6\times 10^{-8}$ | $4.2\times 10^{-9}$ |
| Conductometric biosensor [17] | 1.5-300 ($\times 10^{-6}$) | $Y = 2.5262 + 4.6\times 10^{-5} X$ | 0.9978 | | $5.4\times 10^{-7}$ | |
| Gas sensor [18] | 15 -185 ($\times 10^{-6}$) | $Y = 0.227 + 1.72\times 10^{-7} X$ | 0.9918 | | $5 \times 10^{-6}$ | |
| Low-temperature sensor [19] | 1–5 ($\times 10^{-6}$) | | 0.9998 | | $1 \times 10^{-6}$ | |
| Miniature room temperature sensor [20] | 1−30 ($\times 10^{-6}$) | | | | $1 \times 10^{-6}$ | |

3.4 Selectivity of the sensor

For the system containing 8.0 ng HCHO $mL^{-1}$ and 8.0 ng HCHO $mL^{-1}$ + X (μg coexistent materials $mL^{-1}$), the allowed multiples of coexistent materials were determined by this sensor and resonance fluorescence spectrometry [11]. When the relative error (Er) was ± 5%, the allowed multiples of coexistent materials in water samples were compared with those in Ref. [11] (0.50 μg HCHO $mL^{-1}$), and the results are listed in **Table S1**.

Citric acid, phenol, acetone, methanol, acetaldehyde and oxalic acid are commonly encountered organic compounds (OCs) in water samples. A good formaldehyde sensor should exhibit little response

to these OCs other than formaldehyde to avoid false signal. As shown in **Table S1**, Resonance fluorescence spectrometry exhibit response for these OCs, which results in strong interference to the detection of formaldehyde. The AuNRs colorimetric sensor only shows very weak response to these Ocs, common metal cations and inorganic anions, showing high selectivity of this sensor. The reason is that the fast response of the sensor to HCHO.

3.5. Analysis of samples

In order to demonstrate the practicality of this colorimetric sensor, acidic digestion of real samples was performed according to Ref. [53]. Briefly, 10.00 mL water samples of different Jiulong river section and tap water were treated with 5.00 mL of 65% $HNO_3$ and boiled for 20 min to remove coexisting organic substances and convert $Fe^{2+}$ to $Fe^{3+}$, respectively. The pH of the residual solution was adjusted to 9.58 with NaOH-glycine buffer and heated again for 20 min to precipitate $Fe^{3+}$, $Cr^{3+}$ and $Cu^{2+}$. Then the treated water samples were filtered with 0.45 μM membranes to remove the impurities and the solution was diluted to 100 mL with water before used.

1.00 mL sample solution was taken and the concentration of HCHO was detected using the AuNRs-$Ag^{+}$ sensor. Simultaneity, the standard recovery experiment was also carried out. The results were compared with those obtained by SSRTP and listed in **Table 3-4.**

**Table 3** Determination of HCHO in water samples

| | AuNRs colorimetric sensor (n = 6.) | | | | SSRTP (n = 5.) | |
|---|---|---|---|---|---|---|
| Samples | Medium value (ng $mL^{-1}$) | Addition (ng $mL^{-1}$) | Recovery (%) | RSD (%) | Medium value (ng $mL^{-1}$) | Er (%) |
| River water | 392.0 | 40 | 101 | 2.5 | 387.4 | 1.2 |
| Tap water | 29.5 | 15 | 98.6 | 3.7 | 30.3 | –2.6 |

**Table 4** Analysis of the significant differences for determination results (P = 90%, $f = n_1 + n_2 - 2 = 9$, $F_{0.90, 9} = 6.3$, $t_{0.90, 9} = 1.8$)

| Sample | AuNRs colorimetric sensor (ng $mL^{-1}$, $n = 6$) | SSRTP (ng $mL^{-1}$, $n = 5$) | Statistical analysis |
|---|---|---|---|

| | $\overline{X}_1$ | $S_1$ | $\overline{X}_2$ | $S_2$ | F | $\overline{S}$ | t |
|---|---|---|---|---|---|---|---|
| River water | 392.0 | 4.3 | 387.4 | 4.6 | 1.1 | 4.5 | 1.7 |
| Tap water | 29.5 | 1.2 | 30.3 | 1.8 | 2.4 | 1.5 | 0.80 |

As shown in **table 3**, the content of HCHO in water samples was obtained by AuNRs colorimetric sensor accorded with those obtained by SSRTP. It shows that the HCHO content of river water was higher than that of tap water, we could forecast that river water may be contaminated. Thus, this method could be applied to determination of HCHO content in water samples and prediction of formaldehyde pollution.

Seen from **Table 4**, the F was 1.1 and 2.4 for the three water sample, respectively, indicating that there was no significant differences between $S_1$ and $S_2$, and the corresponding t was 1.7 and 0.8, respectively, indicating that there was also no significant differences between $\overline{X}_1$ and $\overline{X}_2$. Obviously, the results of the proposed sensor were tallied well with those obtained by SSRTP, indicating that the designed sensor was sensitive, accurate and reliable to the detection and monitor of HCHO in the environment.

## 4. Conclusion

Ultra-sensitive AuNRs colorimetric sensor for the determination of HCHO has been developed based on the obvious change of $\Delta\lambda_{LPAB}$ in AuNRs-$Ag^+$-glycine-sodium hydroxide buffer-HCHO system. This sensor exhibited many merits, such as rapid response, wide linear range, simple operation and without surface modification, which is suitable for on-site analysis of HCHO in real samples with low content. This study provides a new way for the design of AuNRs colorimetric sensor, and it also has an important effect on the development and application of the colorimetric sensors, possessing a potential application prospect for protecting human health and better surviving environment for human.

## Acknowledgements

This work was supported by Fujian Province Natural Science Foundation (Grant No. 2013Y0081,

2012D137, 2012H6026), Fujian Province Education Committee (JA11311, JA12207), Fujian provincial bureau of quality and technical supervison (FJQI 2011006), Zhangzhou Natural Science Foundation (ZZ2014J01**)** and Scientific Research Program of Zhangzhou Institute of Technology Foundation (ZZY1215, ZZY 1417). At the same time, we are very grateful to precious advices raised by the anonymous reviewers.

**Reference**

[1]. Q. Li, M. Oshima, S. Motomizu, *Talanta*, 2007, **72**, 1675–1680.

[2]. T. Salthammer, S. Mentese, R. Marutzky, *Chem. Rev*., 2010, **110**, 2536–2572.

[3] A. Allouch, M. Guglielmino, P. Bernhardt, CA. Serra, S. Le Calvé, *Sensor. Actuat. B. Chem*., 2013, **181**, 551–558.

[4]. Z. Zhang, C. Zhao, Y. Ma, G. Li, *Analyst*, 2014, **139**,3614–3621.

[5]. T. Wang, X. Gao, J. Tong, L. Chen, *Food Chem*., 2012, **131**, 577–1582.

[6] L. Wang, C. L. Zhou, H. Q. Chen, J. G. Chen, J. Fu, B. Ling, *Analyst,* 2010, **135**, 2139–2143.

[7] V. P Uralets, J. A. Rijks, P. A. Leclercq, *J. Chromatogr*, 1980, **194**, 135-138.

[8] Z. Q. Zhang, H. T. Yan, X. F. Yue, *Microchimi. Acta.,* 2004, **146**, 259-263.

[9] M. Yang, X. G. Zhang, H. L. Li, *Analyst*, 2001, **126**, 676-678.

[10] J. M. Liu, T. L. Yang, G. H. Zhu, H. L. Chen, P. P. Li, X. Lin, X. M. Huang. *Spectrochim. Acta. A.,* 2008, **69**, 1004–1009.

[11] G. H. Tan, G. R. Li, J. Zhou, *Chin. J. Spectrosc. Lab*., 2010, **27**, 1436-1439.

[12]. S. Han, J. Wang, S. Jia, *Microchim Acta*, 2014, **181**,147–153.

[13]. N. Sugaya, T. Nakagawa, K. Sakurai, M. Morita, S. Onodera, *J. Health Sci*., 2001, **47**,21–27.

[14] G. R. Li, L. J. Han, *Anal. Methods*, 2014, **6**, 426–432.

[15] P. Y. Ma, F. H. Liang, D. Wang, Q. Q. Yang, Y. Y. Ding, Y. Yu, D. J. Gao, D. Q. Song, X. H. Wang, *Microchim Acta*, 2015, **182**, 863–869.

[16] J. Ch. Zhao, G. L Wang, T. Cao, Zh. Guo, *Food Anal. Methods*, 2015, DOI 10.1007/s12161-015-0183-x

[17] N. B. Thanh-Thuy, S. Joëlle, J. R. Nicole, *Anal. Bioanal. Chem.*, 2014, **406**,1039–1048

[18] N. Wang, X. F. Wang, Y. T. Jia, X. Q. Li , J. Y. Yu , B. Ding, *Carbohyd. Polym*. 2014, **108,** 192–199.

[19] R Pandeeswari, B. G. Jeyaprakas, *Bull. Mater. Sci.,* 2014, **37**, 1293–1299.

[20] X. H. Chang, M. Peng, J. F. Yang, T. Wang, Y. liu, J. Zheng, X. G. Li, *RSC Adv*., 2015, **5**, 75098–75104

[21]. K. Saha, S. S. Agasti, C. Kim, X. Li, V. M. Rotello, *Chem. Rev.* 2012, **112**, 2739−2779.

[22]. D. Liu, Z.Wang, X. Jiang, *Nanoscale*, 2011, **3**, 1421−1433.

[23]. G. Wang, Y.Wang, L.Chen, J.Choo, Biosens. Bioelectron. 2010, **25**, 1859−1868.

[24]. M. Coronado-Puchau, L. Saa, M. Grzelczak, V. Pavlov, L. M. Liz-Marzan, *Nano Today*, 2013, **8**,

461–468.

[25]. J. Perez-Juste, I. Pastoriza-Santos, L. M. Liz-Marzan, P. Mulvaney, *Coord. Chem. Rev*., 2005, **249**, 1870–1901.

[26] V. Sharma, K. Park, M. Srinivasarao, *Mater. Sci. Eng. R.*, 2009, **65**, 1-38.

[27] H. Y. Wu, W. L. Huang, M. H. Huang. *Cryst. Growth Des*., 2007,**7**, 831-835.

[28] X. C. Ye, L. H. Jin, H. Caglayan, J. Chen, G. Z. Xing, C. Zheng, V. Doan-Nguyen, Y. J. Kang, N. Engheta, C. R. Kagan, C. B. Murray, *Nano*., 2012, **6**, 2804-2817.

[29] S. K. Ghosh, T. Pal, *Chem. Rev*., 2007,**107**, 4797-4862.

[30] X. L. Ren, L. Q. Yang, J. Ren, *Nanoscale Res. Lett*., 2010, **5**, 1658-1663.

[31] R. Matthew, E. H. Florencio, D. C. Andres, *Anal. Chem*., 2006, **78**, 445-451.

[32] F. M. Li, J. M. Liu, X. X. Wang, L. P. Lin, W. L. Cai, Y. N. Zeng, L. H. Zhang, S. Q. Lin, *Sens.Actuators, B. Chem.*, 2011, **155**, 817-822.

[33] N. Xiao, C. X. Yu, *Anal. Chem.,* 2010, **82**, 3659-3663.

[34] J. M. Liu, X. X. Wang, F. M. Li, L. P. Lin, W. L. Cai, X. Lin, L. H. Zhang, Z. M. Li, S. Q. Lin, *Anal Chim Acta*., 2011, 708, 130-133.

[35] C.V. Durgadas, V. N. Lakshmi, C.P. Sharma, K. Sreenivasan, *Sens. Actuators, B. Chem*., 2011, **156**, 791-797.

[36] J. M. Liu, L. Jiao, M. L. Cui, L. P. Lin, X. X. Wang, Z. Y. Zheng, L. H. Zhang, S. L. Jiang, *Sens. Actuators B*., 2013, 188, 644-650.

[37] J. M. Liu, L. Jiao, L. P. Lin, M. L. Cui, X, X, Wang, L. H. Zhang, Z. Y. Zheng, S. L. Jiang, *Talanta*, 2013,**117**, 425–430.

[38] J. M. Liu, X. X. Wang, L. Jiao, M. L. Cui, L. P. Lin, L. H. Zhang, S. L. Jiang, *Talanta*, 2013, **116**, 199–204.

[39] Zh. Y. Zhang, Zh. P. Chen, D. W. Pan, L. X. Chen, *Langmuir*, 2015, **31**, 643−650.

[40] P. K. Sudeep, S. T. S. Joseph, K. G. Thomas, *J. Am. Chem. Soc*., 2005, **127**, 6516-6517.

[41] J. M. Liu, L. Jiao, M. L. Cui, L. P. Lin, X. X. Wang, Z. Y. Zheng, L. H. Zhang, S. L. Jiang, *Sens. Actuators B*., 2013,**188**, 613-620.

[42] J. M. Liu, X. X. Wang, M. L. Cui, L. P. Lin, S. L. Jiang, L. Jiao, L. H. Zhang, *Sens. Actuators B*., 2013, **176**, 97-102.

[43] X. X. Wang, J. M. Liu, S. L. Jiang, L. Jiao, L. P. Lin, M. L. Cui, X. Y. Zhang, L. H. Zhang, Z. Y.

Zheng, *Sens. Actuators B*., 2013,**182**, 205– 210.

[44] Y. Sh. Wang, D. H Zhang, W. Liu, X. Zhang, Sh. X. Yu, T. Liu, W. T. Zhang, W. X. Zhu, J. L. Wang, *Biosens. Bioelectron*., 2014, **55**, 242–248.

[45] L. L. Lu, Y. Sh. Xia, *Blood.Anal. Chem*., 2015, **87**, 8584−8591.

[46]. L. Saa, M. Coronado-Puchau, V. Pavlov, L. M. Liz-Marz´an, *Nanoscale*, 2014, **6**, 7405–7409.

[47] H. Lee, S. M. Dellatore, W. M. Miller, P. B. Messersmith., *Sci*., 2007, **318**, 426-430.

[48] R. Liu, T. S. Zhong, C. X. Lei., *Chem. Sens*., 2011, **31**, 10-16.

[49] C. C. Huang, Z. S. Yang, H. T. Chang., Langmuir, 2004, **20**, 6089-6092.

[50] M. Grzelczak, J. Perez-Juste, F. J. G. De Abajo, L. M. J. Liz-Marzán., *Phys. Chem. C*, 2007, **111**: 6183-6188.

[51] Y. R. Ma, H. Y. Niu, X. l. Zhang, Y. Q. Cai, *Analyst*, 2011, **136**, 4192-4196.

[52] Q. Cao, H. Zhao, Y. J. He, X. J. Li , Li. X. Zeng, N. Ding, J. Wang, J. Yang, G. W. Wang, *Biosens.. Bioelectron*., 2010,**25**, 2680–2685.

[53] O.D. Uluozlu, M. Tuzen, D. Mendil, B. Kahveci, M. Soylak, *J. Hazard. Mater.* 2009, **172**, 395–399.

.